A FEM Simulation of the Eddy Current Losses in Thin Ferromagnetic Sheets

Karl Hollaus and Oszkár Bíró

***Abstract*--A part of a concept to treat eddy currents in thin ferromagnetic sheets and the associated losses is presented. To circumvent the cumbersome modeling of the sheets individually by the Finite Element Method (FEM), the conducting region is considered as a bulk for which a proper overall field solution is given. Based on the solution above, the laminations are taken into account by a one dimensional model considering hysteresis nonlinearity by the classical scalar Preisach model. A novel technique to treat the hysteresis nonlinearity will be introduced. Some preliminary results are presented.**

***Index Terms*--Finite element method, thin ferromagnetic sheets, anisotropic conductivity, hysteresis.**

I. Introduction

The purpose of laminating iron cores in electric devices is the reduction of the eddy current losses. Therefore, the simulation of the eddy current distribution in laminated iron with almost arbitrary complicated geometry is not only an interesting and challenging task in the numerical simulation of electromagnetic fields but also of great practical importance.

It can be stated that the simulation of eddy currents of three dimensional arrangements with complex geometry even in isotropic ferromagnetic materials with pronounced saturation effects can be solved routinely [1].

Modeling of the sheets individually by the FEM leads to extremely high computational costs, therefore, it doesn't represent a feasible solution for practical problems. Such modeling may serve for verification of approximate techniques at best.

To overcome this unpleasant limitation, many efforts have been already undertaken. The models developed simulate on the one hand an overall field distribution only by applying either a single component current vector potential [2] or an anisotropic conductivity [3]. On the other hand, 1-D models [4] or 2-D models [5] take account of the small eddy current loops caused by the main magnetic flux parallel to the laminations. Both models fail an exact simulation of the eddy current distribution in laminations.

Manuscript received September 20, 2000.

This work was supported by the "Fonds zur Förderung der wissenschaftlichen Forschung", Vienna, Austria under the Grant No. P 13551-TEC.

Karl Hollaus, is with the IGTE, Technical University of Graz, Kopernikusgasse 24, A-8010 Graz, Austria (telephone: +43 316 873 7259, e-mail hollaus@igte.tu-graz.ac.at).

Oszkár Bíró, is with the IGTE, Technical University of Graz, Kopernikusgasse 24, A-8010 Graz, Austria (telephone: +43 316 873 7263, e-mail biro@igte.tu-graz.ac.at).

II. Different Types of Eddy Currents

To simplify the subsequent explanations, the eddy currents occurring in a single lamination are split up into two different types. The large eddy current loops $\mathbf{J}_s$ are caused by the stray field $\mathbf{\Phi}_s$ which penetrates the lamination with an appreciable normal component. Due to the main magnetic flux $\mathbf{\Phi}_m$ which is parallel to the lamination, extremely narrow eddy current loops $\mathbf{J}_m$ are generated.

Eddy Currents: Magnetic stray field $\mathbf{\Phi}_s \rightarrow \mathbf{J}_s$

Main magnetic field $\mathbf{\Phi}_m \rightarrow \mathbf{J}_m$

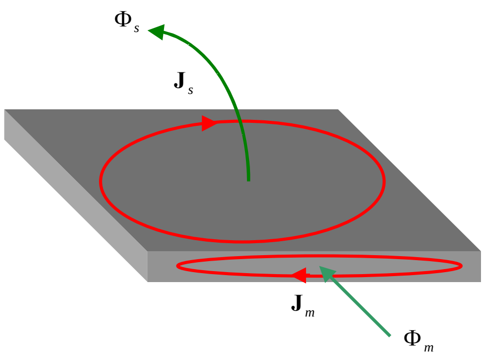

Fig. 1. Single lamination with eddy currents.

In the first step, the large eddy current loops are simulated by a single current vector potential $\mathbf{T}$ or an anisotropic conductivity. This results in the overall field distribution.

The application of an anisotropic conductivity has been studied on a simple model comprehensively [6]. Both an anisotropic conductivity in order to obtain a feasible overall field distribution and a model taking account of each lamination have been investigated. A comparison of the results obtained has been carried out. The obtained results have shown that, choosing a feasible anisotropy, the overall field distributions of the magnetic field as well as the eddy currents agree quite well with each other within the volume and also on the surface.

In a previous work [7] a method for the linear case has been developed which is capable to simulate the large eddy current loops caused by the magnetic stray field by treating the core as a bulk of a material with anisotropic conductivity in a three dimensional model. In a second step, the small eddy current loops due to the main magnetic flux have been considered. Each laminate is taken into account by writing the field components in it as fundamental solutions of the diffusion equation so that the averages of the tangential electric and magnetic field components over the thickness of the sheet equal the averages obtained in the first step.

In the present work the above concept is attempted to be generalized to thin ferromagnetic sheets considering hysteresis to simulate the eddy currents and the associated losses in an efficient and resource saving way.

III. One Dimensional Model of Hysteresis

Once the overall field distribution is determined, the narrow eddy current loops due to the main magnetic field have to be reconstructed. To this end, a rather simple model should suffice. In the following section, the mathematical model is derived.

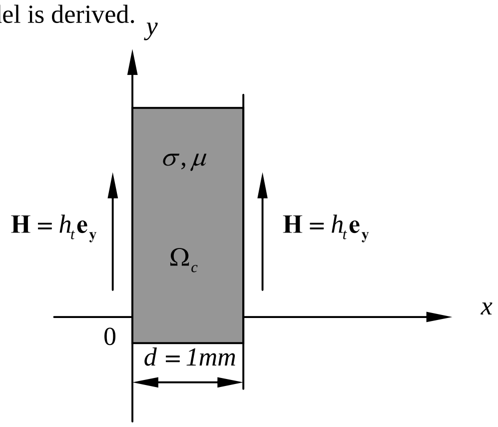

Fig. 2. One dimensional model with one lamination.

The model is represented in Fig. 2. It consists of one lamination and is one dimensional. Hysteresis nonlinearity is considered by the classical scalar Preisach model [8]. The eddy current problem, i.e., the low frequency subset of Maxwell's equations, neglecting the displacement current density, is formulated preliminarily in terms of the magnetic field intensity $\mathbf{H}$ using nodal elements. On both sides of the lamination, the tangential component of the magnetic field intensity $\mathbf{H}$ is prescribed. Hence, a system of partial differential equations is valid in the conducting region

$$curl\mathbf{H} = \mathbf{J} \tag{1}$$

$$curl\mathbf{E} = -\frac{\partial \mathbf{B}}{\partial t} . \tag{2}$$

On the boundary, the tangential component

$$\mathbf{H} = \mathbf{H_t} \tag{3}$$

is prescribed. From (1) and (2), the partial differential equation

$$curl\rho curl\mathbf{H} = -\frac{\partial}{\partial t}\mu\mathbf{H} \tag{4}$$

is obtained in the conducting region after considering

$$\mathbf{E} = \rho\mathbf{J} , \tag{5}$$

$$\mathbf{B} = \mu\mathbf{H} . \tag{6}$$

To solve the partial differential equation in (4) the method of Galerkin for finite elements is employed. To this end, the unknown field value $\mathbf{H}$ is approximated by vector shape functions

$$\mathbf{H} \approx \mathbf{H}^{(n)} = \sum_{k=1}^{n^{(node)}} \left(h_{xk}\mathbf{N}_{xk} + h_{yk}\mathbf{N}_{yk} + h_{zk}\mathbf{N}_{zk} \right). \tag{7}$$

The vector shape functions can be written as

$$\mathbf{N}_{xk} = N_k\mathbf{e}_x ,\ \mathbf{N}_{yk} = N_k\mathbf{e}_y \text{ and } \mathbf{N}_{zk} = N_k\mathbf{e}_z . \tag{8}$$

Here N_k represents a scalar nodal shape function. To minimize the error due to the approximation, the residual is weighted by the same vector shape functions over the conducting region Ω_c

$$\int_{\Omega_c} \mathbf{N}_i (curl\rho curl\mathbf{H}^{(n)} + \frac{\partial}{\partial t}\mu\mathbf{H}^{(n)}) d\Omega = \mathbf{0} , \tag{9}$$

whereby $\mathbf{N}_i$ means

$$\mathbf{N}_i = N_i\mathbf{e}_x + N_i\mathbf{e}_y + N_i\mathbf{e}_z . \tag{10}$$

After exploiting the vector identity

$$\int_{\Omega_c} \mathbf{U} curl\rho curl\mathbf{V} d\Omega = \int_{\Omega_c} curl\mathbf{U}\rho curl\mathbf{V} d\Omega - \oint_{\Gamma} \mathbf{U} \times \rho curl\mathbf{V} d\Omega \tag{11}$$

the double derivation of the unknown field value $\mathbf{H}^{(n)}$ in (9) can be avoided.

$$\int_{\Omega_c} (curl\mathbf{N}_i \rho curl\mathbf{H}^{(n)} + \mathbf{N}_i \frac{\partial}{\partial t}\mu\mathbf{H}^{(n)}) d\Omega - \oint_{\Gamma} \mathbf{N}_i \times \rho curl\mathbf{H}^{(n)} d\Omega = \mathbf{0} \tag{12}$$

Since the shape functions $\mathbf{N}_i$ have to fulfill the required homogenous Dirichlet boundary conditions

$$\mathbf{N}_i \times \mathbf{n} = \mathbf{0} \tag{13}$$

the surface integral in (12) vanishes. Hence,

$$\int_{\Omega_c} (curl\mathbf{N}_i \rho curl\mathbf{H}^{(n)} + \mathbf{N}_i \frac{\partial}{\partial t} \mu \mathbf{H}^{(n)}) d\Omega = \mathbf{0} \quad (14)$$

is obtained. The description of the problem shall be scalar

$$\mathbf{H} = h_y \mathbf{e}_y \quad (15)$$

and one dimensional

$$\frac{\partial}{\partial y} = 0 \, , \; \frac{\partial}{\partial z} = 0 \, . \quad (16)$$

The unknown field value h_y in (15) is approximated by scalar shape functions

$$h_y \approx h_y^{(n)} = \sum_{k=1}^{n^{(node)}} h_{yk} N_k \, . \quad (17)$$

Thus,

$$\int_x (\frac{\partial}{\partial x} N_i \rho \frac{\partial}{\partial x} h_y^{(n)} + N_i \frac{\partial}{\partial t} \mu h_y^{(n)}) dx = 0 \quad (18)$$

is valid in the conducting region Ω_c and

$$x = 0 \quad ... \; h_y^{(n)} = h_t \quad (19)$$

$$x = d \quad ... \; h_y^{(n)} = h_t \quad (20)$$

on the boundary Γ. After integrating (18) and taking account of the known inhomogeneous Dirichlet boundary conditions (19) and (20) the description of the model ends up in a system of inhomogeneous ordinary differential equations

$$[\mathbf{A}]\{\mathbf{h}(t)\} + \frac{\partial}{\partial t}([\mathbf{B}(\mathbf{h})]\{\mathbf{h}(t)\}) = \mathbf{r}(t) \, . \quad (21)$$

The vector $\{\mathbf{h}(t)\}$ in (21) represents the unknown nodal values of $h_y^{(n)}$ in (18), the mass matrix $[\mathbf{B}(\mathbf{h})]$ comprises the nonlinear material property indicated by it's dependency on $(\mathbf{h})$. Finally, the system of inhomogeneous ordinary differential equations (21) will be solved by a time stepping scheme.

IV. Treatment of the Hysteresis Nonlinearity

There are various existing methods, for instance, the fixed point technique [10] to treat the hysteresis nonlinearity. A novel alternative technique to achieve fast convergence of the time stepping scheme has been developed in this paper.

Let us assume that the solution at an arbitrary point in the problem region is sought for the next time step. The solution must lie either on a B-H curve valid for increasing magnetic field intensity H, (positive B-H curve), or on a B-H curve valid for decreasing magnetic field intensity H, (negative B-H curve), see Figs. 3 and 4. Both branches are known a priori and can be easily computed from the Preisach model taking account of the corresponding history. Therefore, the hysteresis nonlinearity is reduced to a univalent function.

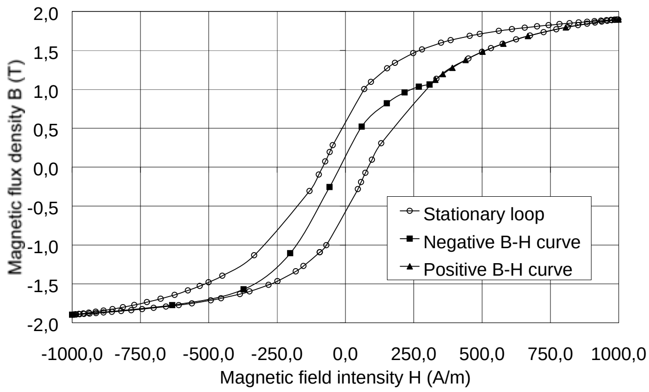

Fig. 3. Stationary loop and B-H curves from the Preisach model inside the area restricted by the limiting triangle.

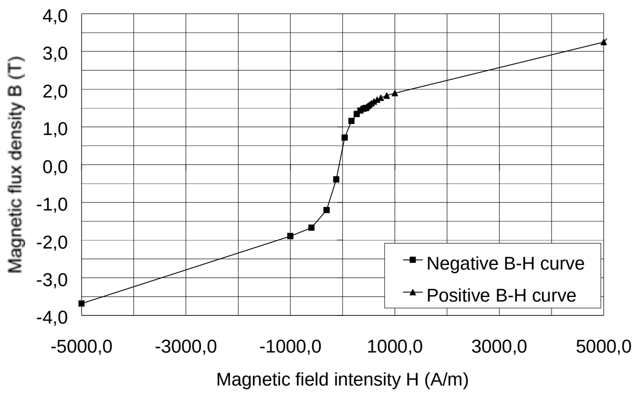

Fig. 4. Stationary loop and B-H curves from the Preisach model inside the area restricted by the limiting triangle.

To take care of the case that a solution lies temporarily outside the area restricted by the limiting triangle of the Preisach model [8], the branches of the B-H curves are extended up to an almost arbitrary large scale. The slope of the extensions has been chosen slightly smaller than that within the permissible area and adjacent to the limit to ensure fast convergence as depicted in Fig. 5.

Experience has shown, that one branch of the B-H curves corresponding to the Preisach distribution function used [9] is convex, whereas the other branch is in the first part concave and later on convex. In [10] it has been elaborated extensively how to proceed in order to achieve a stable

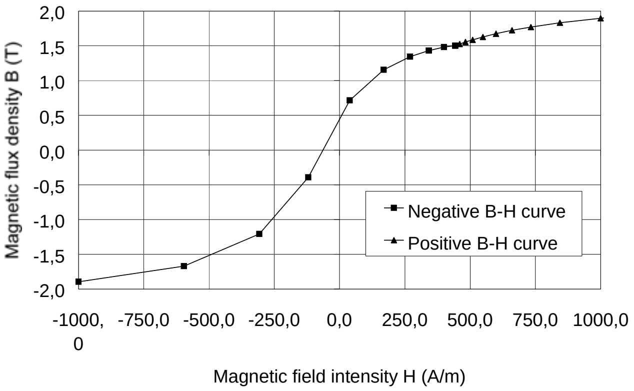

Fig. 5. B-H curves from the Preisach model inside and outside the area restricted by the limiting triangle.

scheme of nonlinear iteration steps. In the i-th iteration step, the magnitude of H_i yields B_{i+1} from the B-H curve, sketched in Fig. 6. From the secant B_{i+1}/H_i the new permeability μ_{i+1} is computed. In fact, this is convergent without underrelaxation provided the B-H curve is monotonous and convex (i.e. $\partial B/\partial H > 0$ and $\partial^2 B/\partial^2 H < 0$).

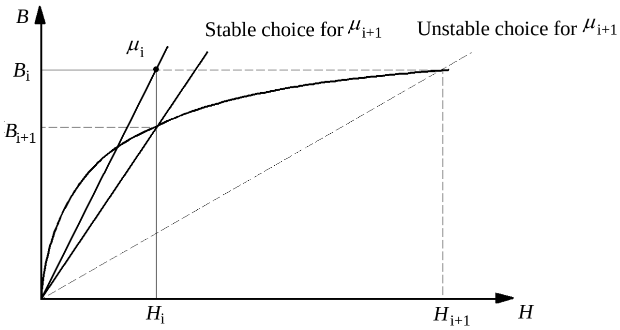

Fig. 6. Scheme of nonlinear iteration step for convex B-H curve

To ensure convergence without underrelaxation even in the
case where the B-H curve is partially concave (i.e. $\partial^2 B/\partial^2 H > 0$), as shown in Fig. 7, a slight modification has to be undertaken in the section, where the curve is concave.

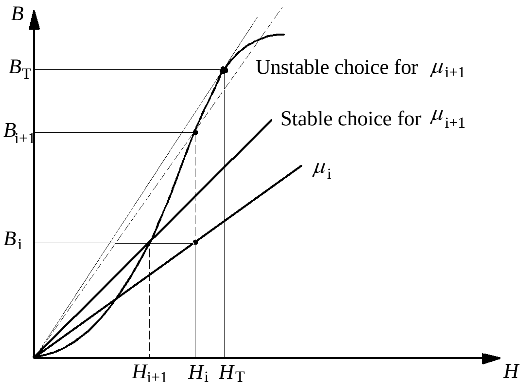

Fig. 7. Scheme of nonlinear iteration step for concave magnetizing curve

The magnitude H_i is multiplied by the previous value of the permeability μ_i which yields B_i. From the B-H curve H_{i+1} is calculated, the new permeability is the secant B_i/H_{i+1}.

The iteration process is terminated once the variation in the permeability between two iteration steps becomes small enough.

A few points for the branches of the B-H curves have to be calculated only once for all nonlinear iteration steps. The cost involved is small compared with that needed when the points of the B-H curve are calculated for each nonlinear iteration step directly from the Preisach model.

The hysteresis nonlinearity is considered in terms of the magnetic permeability (18). Therefore it can be incorporated in the FEM quite easily. The element matrices of the FEM are updated at each nonlinear iteration step. Moreover, the treatment of the hysteresis nonlinearity does not need a derivation of the B-H curve and it is convergent even in case of inflection points.

V. Results

A typical soft magnetic material with a coercive field of $H_c = 80A/m$ and a remanent magnetization of $M_r = 0.65Vs/m^2$ was used [9].

First, the influence of hysteresis nonlinearity on the shape of the time function of the magnetic flux density in the middle of the lamination with increasing magnitude of the prescribed tangential component of the magnetic field intensity h_t on the boundary was investigated. The results are represented in Fig. 8 and Fig. 9. The applied frequency was 50Hz. Due to the saturation all curves of the magnetic flux density are flattened and show a characteristic delay with respect to the magnetic field intensity, which is sketched normalized as reference.

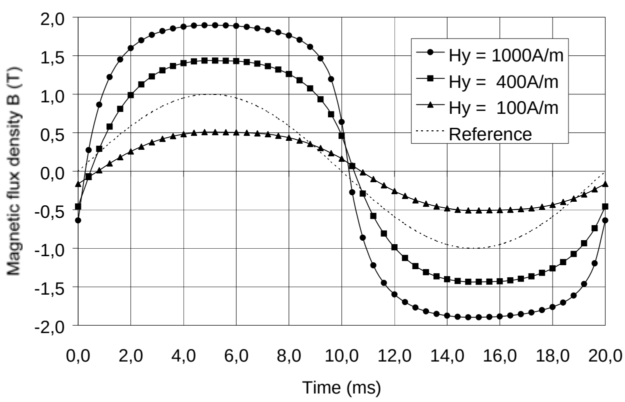

Fig. 8. Magnetic flux density with respect to time without eddy currents.

In case of eddy currents, it can be easily observed in Fig. 9 that the curves demonstrate an appreciably larger deformation as well as delay.

Next, the dependence of the hysteresis losses on the

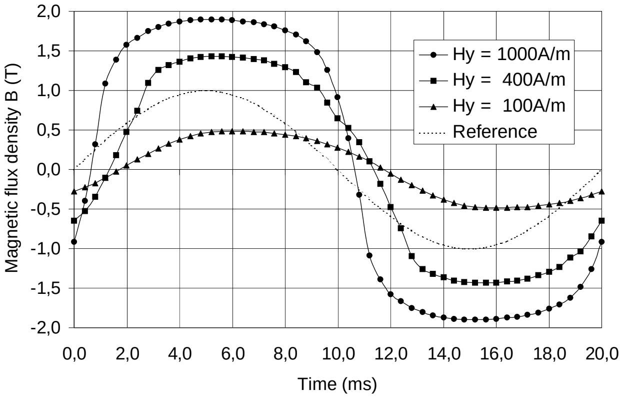

Fig. 9. Magnetic flux density with respect to time with eddy currents.

prescribed boundary conditions are analyzed. Fig. 10 shows the results with and without eddy currents which are close to each other, because equal tangential components h_t on both sides of the lamination are assumed.

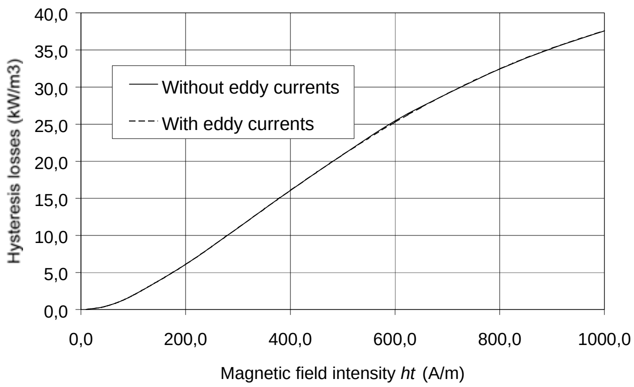

Fig. 10. Hysteresis losses with and without eddy currents.

The computed eddy current losses exhibit an extraordinary behavior. At the beginning the losses increase slightly with respect to the magnitude of the tangential component of the magnetic field intensity h_t. Then, the losses rise steeply. Subsequently, the eddy current losses obey a straight line approximately.

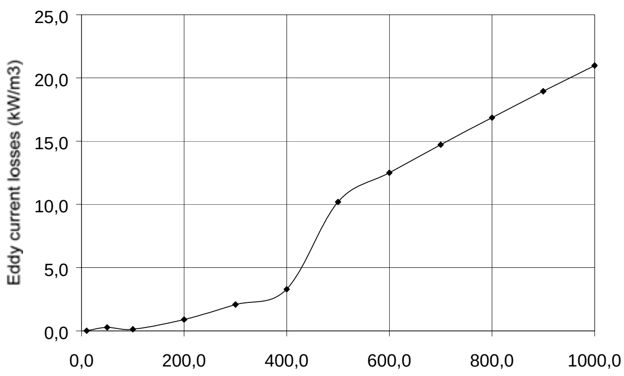

Fig. 11. Eddy current losses with hysteresis.

A comparison of these eddy current losses with those obtained by an ordinary nonlinear material property, i.e., the initial curve of the same material represented in Fig. 12, shows a substantially different characteristic (Fig. 13).

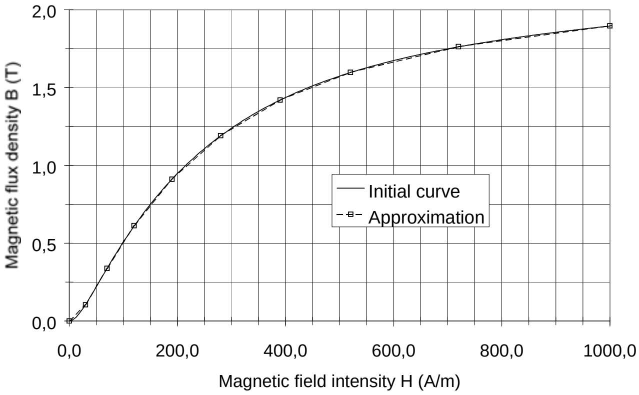

Fig. 12. Initial curve and approximation.

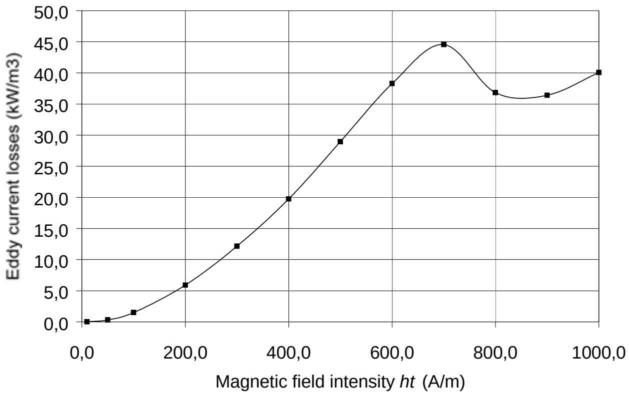

Fig. 13. Eddy current losses without hysteresis (initial curve).

VI. Conclusion

Part of a concept to simulate the eddy current distribution and the associated losses in thin ferromagnetic sheets was presented. An attractive alternative method to handle the hysteresis nonlinearity in an efficient and resource saving way has been introduced. Some preliminary results have been shown.

VII. References

[1] Biro, O., Preis, K., Richter, K. R.: "Various FEM formulations of transient 3d eddy currents in nonlinear media", presented at *CEFC*, Aix-les-Bains, France, July 5-7, 1994, (invited paper), *IEEE Trans. Magn.*, vol. MAG-31, pp. 1307-1312, May 1995.

[2] A. G. Jack, B. C. Mecrow, "Calculation of three-dimensional electromagnetic fields involving laminar eddy currents", *IEE Proceedings*, vol. 134, Pt. A, pp. 663-671, September 1987.

[3] Viviane Cristine Silva, Gérard Meunier, Albert Foggia, "A 3-D Finite-Element Computation of Eddy Currents and Losses in Laminated Iron Cores Allowing for Electric and Magnetic Anisotropy", *IEEE Transactions on Magnetics*, vol. 31, pp. 2139-2141, May 1995.

[4] Jian. G. Zhu, S. Y. R. Hui, V. S. Ramsden, "A Generalized Dynamic Circuit Model of Magnetic Cores for Low- and High-Frequency Applications – Part I: Theoretical Calculation of the Equivalent Core

Losses Resistance", *IEEE Transactions on Power Electronics*, vol. 11, pp. 246-250, March 1993.

[5] L. Luk, G. E. Dawson, A. R. Eastham, "Finite element and difference analysis of losses in laminated material", *IEEE Transactions on Magnetics*, vol. 24, pp. 2679-2681, November 1988.

[6] K. Hollaus, O. Bíró, “Estimation of 3D eddy currents in conducting laminations by an anisotropic conductivity and a 1D analytical solution”, *COMPEL*, vol. 18, no. 3, pp. 494-503, 1999.

[7] Hollaus, K., Biro, O.: "A FEM Formulation to Treat 3D Eddy Currents in Laminations ", presented at *COMPUMAG '99*, Sapporo, Japan, October 24-28, 1999, to be published in *IEEE Trans. Magn.*, vol. MAG-36, September 2000.

[8] Mayergoyz, I. D.: "Mathematical Models of Hysteresis", Springer-Verlag New York, 1991.

[9] Akpinar A. S., Nasar, S. A.: "Parametric analysis of ferroresonace, including hysteresis effects", Electric Machines and Power Systems, vol.18, pp. 473-493, 1990.

[10] Bottauscio, O., Chiampi, M., Chiarabaglio, D., Repetto, M.: " Preisach-type hysteresis models in magnetic field computation ", Physica-B, vol.275, pp.34-39, Jan. 2000.

[11] Biro, O. and Preis, K.: „Finite element calculation of time-periodic 3d eddy currents in nonlinear media“, in T. Honma (ed.), Advanced Computational Electromagnetics, Selected papers of the 3rd Japan-Hungary Joint Seminar on Applied Electromagnetics in Materials and Computational Technology, Budapest, Hungary, 10-13 July, 1994, pp. 62-74, Elsevier, 1995.